Fracture Mechanisms of Polymer Interfaces Reinforced with Block Copolymers: Transition from Chain Pullout to Crazing

Junichiro Washiyama,[†,‡,§] Edward J. Kramer,[*,‡,§] and Chung-Yuen Hui[§,∥]

Departments of Materials Science and Engineering and of Theoretical and Applied Mechanics and Materials Science Center, Cornell University, Ithaca, New York 14853

Received July 29, 1992; Revised Manuscript Received January 7, 1993

ABSTRACT: We have investigated the fracture toughness and fracture mechanisms of planar interfaces between polystyrene (PS) and poly(2-vinylpyridine) (PVP), which were reinforced with a deuterium-labeled dPS/PVP block copolymer, which has a long dPS block (polymerization index $N_{dPS} = 580$) and an intermediate length PVP one ($N_{PVP} = 220$). The critical energy release rate of an interfacial crack, G_c (or fracture toughness), was measured as a function of the areal chain density of the block copolymer, Σ, using an asymmetric double cantilever beam geometry. The fracture mechanisms of the interface were studied by transmission electron microscopy (TEM) and forward recoil spectrometry (FRES) which permitted the location of the dPS block to be determined after fracture. At a critical areal chain density, $\Sigma^* = 0.04$ chains/nm^2, a transition in the fracture mechanisms from chain pullout of the PVP block ($\Sigma < \Sigma^*$) to crazing ($\Sigma > \Sigma^*$) followed by fracture of the craze was observed. At this Σ^*, a discontinuous transition in G_c was also observed. G_c linearly increased with increasing Σ when $\Sigma < \Sigma^*$, exhibited a jump of $\sim$10 J/m^2 at $\Sigma = \Sigma^*$, and then remained approximately constant for $\Sigma > \Sigma^*$. Using the transition value of Σ^*, we calculated a static friction coefficient per monomer for the pullout of the PVP block to be $\mathbf{f}_{mono} = 6.3 \times 10^{-12}$ N/monomer.

Introduction

Block copolymers have been widely used to reinforce interfaces between immiscible polymers.[1,2] The reinforcement mechanism is believed to be "stitching"; i.e., block copolymer chains form interphase junctions through which stress can be transferred, which results in a substantial reinforcement of the interfaces themselves. For the PS/PVP interfaces where PVP domains were surrounded by a PS matrix, Creton et al.[3] examined this stitching effect of PS/PVP block copolymers and concluded that at least one entanglement between each block and its respective polymer was necessary to achieve effective interfacial reinforcement.

Recently, an asymmetric double cantilever beam method has been developed[4] and applied to measure the fracture toughness of interfaces between immiscible polymers.[5,6] These studies have examined the reinforcement effects of various combinations of block copolymers added to the interfaces between immiscible homopolymers and observed a remarkable improvement in the fracture toughness, G_c, of the interfaces as a function of the polymerization index of both blocks, N, and the areal density of the block copolymer chains, Σ. Concurrently, theoretical models[7-9] have been developed to explain the reinforcement effect of block copolymers at the interfaces between immiscible homopolymers. In addition, a fracture mechanism map for interfaces between immiscible polymers which preferentially deform plastically by crazing was proposed by Xu et al.[9] Part of the fracture mechanism map for PS/PVP interfaces was examined by measurements of the interfacial fracture toughness, forward recoil spectrometry (FRES), Rutherford backscattering spectrometry (RBS), and X-ray photoelectron spectroscopy (XPS) of the fracture surfaces[6,10] as well as cross-sectional transmission electron microscopy (TEM) of thin microtomed slices through the interface.[11]

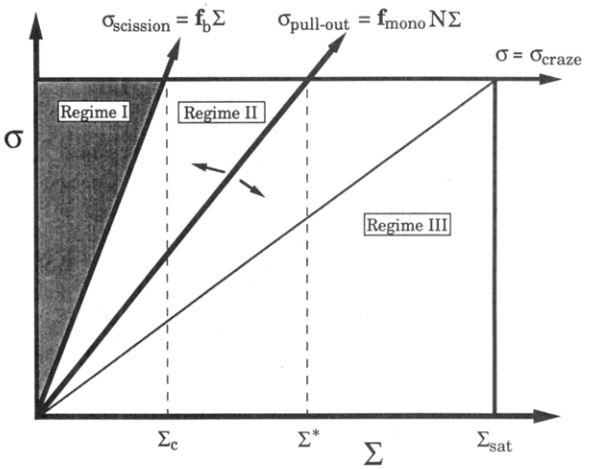

Figure 1. Fracture mechanism map.[9] Note that there are three different regimes I–III, in the fracture mechanis map depending on the magnitude of $\sigma_{pullout}$. In regime I, a fracture mechanism transition from chain scission ($\Sigma < \Sigma_c$) to crazing ($\Sigma > \Sigma_c$) is expected. In regime II, the transition from chain pullout to crazing is expected. Only pullout, and no fracture mechanism transition to crazing, is expected in regime III.

According to the map (see Figure 1), two kinds of fracture mechanism transitions are possible as Σ increases. The first one is the transition from the chain scission to crazing under conditions where $N \gg N_e$ for both blocks, where N_e denotes the polymerization index between entanglements of its respective homopolymer. Previous experimental work[6] on PS/PVP interfaces showed conclusively that this transition exists, and an analysis allowed Creton et al. to estimate the force to break a single block copolymer chain ($\sim 2 \times 10^{-9}$ N/bond).[6] Another transition, however, is possible, one from chain pullout to crazing ($N < N_e$ for one block) if a high enough Σ can be achieved before the interface is saturated with the block copolymer. This second case is particularly important for the molecular design of block copolymers for the reinforcement of interfaces between immiscible polymers. The determination of a minimum polymerization index of a block above which no chain pullout can take place and determination of conditions (N or Σ) for crazing are both crucial to achieve strong interfacial reinforcement. In addition, well-con-

† Visiting scientist from Kawasaki Plastics Laboratory, Showa Denko K.K., 3-2, Chidori-cho, Kawasaki-ku, Kawasaki, Kanagawa 210, Japan.
‡ Department of Materials Science and Engineering.
§ Materials Science Center.
∥ Department of Theoretical and Applied Mechanics.

0024-9297/93/2226-2928$04.00/0

trolled interfacial strength will sometimes become an important issue (easy-peel films for food packaging is a typical example), and, in this case, the chain pullout regime should be the principal subject. Nevertheless, this chain pullout/crazing transition regime has not been quantitatively examined: only the TEM studies of Washiyama et al.[11] qualitatively investigated the fracture mechanism map.

We have chosen polystyrene (PS) and poly(2-vinylpyridine) (PVP) homopolymers as the immiscible polymer pair and dPS/PVP block copolymers to reinforce the interface between PS and PVP. The advantages of this system are reviewed below. First, both homopolymers have nearly the same glass transition temperature and thermal expansion coefficient so that little, if any, thermal stress results during cooling from an annealing temperature where the polymers are molten (necessary to produce good contact and block copolymer organization at the interface). Second, both PS and PVP deform plastically by crazing,[6] which can be investigated using transmission electron microscopy techniques (TEM).[11] The PS phase has a somewhat smaller crazing stress than PVP. Furthermore, thermodynamic characteristics, such as the Flory interaction parameter, χ, between PS and PVP are known from previous studies,[12-14] giving us an additional advantage in understanding this system.

The Fracture Mechanism Map.[9]

Figure 1 shows the fracture mechanism map based on the work by Xu et al.[9] which we have modified by introducing Σ_{sat}, the areal chain density at saturation. The map describes the relationship between the maximum tensile stress, σ, ahead of the crack tip and normal to the interface and the areal density of the block copolymer, Σ, where at least one of the materials is capable of deforming plastically by crazing.

The horizontal line $\sigma = \sigma_{craze}$ represents an upper limit which is independent of Σ, since we assume a craze widens into one polymer phase (in this case PS) under constant stress, σ_{craze}. The vertical line, $\Sigma = \Sigma_{sat}$, provides an upper limit of areal chain density above which the interface becomes saturated with block copolymers so that additional block copolymer chains can no longer organize as a brush at the interface but form other phases, such as micelles or lamellae, near the interface.[12] In the regime $\Sigma > \Sigma_{sat}$, the existence of these phases near the interface may affect G_c and the corresponding interfacial fracture mechanisms which determine G_c, but this regime is beyond the scope of this paper; details of this regime will be discussed separately.[15]

The stress for chain scission and the stress for block pullout both increase from zero linearly with Σ so only one of these fracture mechanisms can operate, the one with the smaller slope on the σ vs Σ map. The stress required to cause chain scission of block copolymer chains at the interface $\sigma_{scission}$ is given by eq 1 where $\mathbf{f}_b$ denotes the force

$$\sigma_{scission} = \mathbf{f}_b\Sigma \tag{1}$$

to break a single C–C bond. (Note that, for the PS/PVP block copolymer all main-chain bonds consist of C–C bonds.) The value of $\mathbf{f}_b$ has been determined from both theoretical[16] and experimental[6,7,17] studies.

The block pullout stress, $\sigma_{pullout}$, arising from the frictional force between the copolymer block and the bulk polymer chains surrounding it, is assumed to be given by eq 2, viz.

$$\sigma_{pullout} = \mathbf{f}_{mono}N\sigma \tag{2}$$

where $\mathbf{f}_{mono}$ denotes a static (velocity-independent) friction coefficient per monomer, and N is the polymerization index of a block which is subjected to pullout. This simple form of eq 2 can only be expected to hold for blocks shorter than N_e; for $N \gg N_e$, $\sigma_{pullout}$ will increase with N more strongly than linearly.

The $\sigma_{pullout}$ line can fall in one of three different regimes depending on the value of N: we define such regimes as I–III as shown in Figure 1 and describe them in detail below.

Regime I. Regime I, corresponding to large N, has been well studied both theoretically and experimentally, and a quantitative foundation has been established. From Figure 1, there is a critical chain density at Σ_c given by eq 3, at which a fracture mechanism transition would be expected.

$$\Sigma_c = \sigma_{craze}/\mathbf{f}_b \tag{3}$$

When $\Sigma < \Sigma_c$, chain scission of the block copolymer chains somewhere near the interface would be the dominant fracture mechanism, since $\sigma_{scission} < \sigma_{craze}$ in this range of Σ. On the other hand, when $\Sigma > \Sigma_c$, crazing would be the dominant mechanism, since $\sigma_{scission} > \sigma_{craze}$. This transition from noncrazing (chain scission) to crazing has indeed been confirmed by the optical microscopic studies of Creton et al.[6] and with the TEM studies of Washiyama et al.[11] It is emphasized that this transition is dictated by the bond strength (for example, C–C bond) and, hence, should be universal.

Brown[5] and Creton et al.[6] measured G_c corresponding to this regime, particularly the crazing situation, and found that G_c scales as $G_c \sim \Sigma^2$, being consistent with the theoretical studies of Brown[7] and Hui et al.[8] Creton et al.[6] have demonstrated that G_c scales as $G_c \sim \Sigma_{eff}^2$, where Σ_{eff} is the number of effectively entangled (load-bearing) chains at the interface.

Regime II. The second regime corresponds to an intermediate N. In this regime, a transition in the fracture mechanism would be expected at Σ^*, given by eq 4, from chain pullout ($\Sigma < \Sigma^*$) to crazing ($\Sigma > \Sigma^*$).

$$\Sigma^* = \sigma_{craze}/\mathbf{f}_{mono}N \tag{4}$$

At this transition, we would expect a discontinuous change in G_c associated with the fracture mechanism transition: G_c will increase linearly with increasing Σ (for $\Sigma < \Sigma^*$) and then would show a jump at $\Sigma = \Sigma^*$. Above the transition, we would expect G_c to increase until the Σ_{eff} saturates. We will focus on a quantitative examination of this regime II in this study.

Regime III. When a block is extremely short, the $\sigma_{pullout}$ cannot exceed σ_{craze} over the entire range of $\Sigma < \Sigma_{sat}$, and hence chain pullout would be the fracture mechanism throughout this whole regime. Creton et al.[6] have examined this regime, and they found that G_c increased linearly with increasing Σ (for $\Sigma < \Sigma_{sat}$) and then saturated, consistent with the prediction of this fracture mechanism map.

The boundaries between the regimes can be given in terms of N, the polymerization index of the shortest block. To be in regime I requires that the slope ($\mathbf{f}_{mono}N$) of the pullout line, σ vs Σ (eq 2), be larger than that ($\mathbf{f}_b$) of the chain-scission line; thus

$$N > \mathbf{f}_b/\mathbf{f}_{mono} \qquad \text{regime I} \tag{5a}$$

or since $\Sigma_c = \sigma_{craze}/\mathbf{f}_b$

$$N > \sigma_{craze}/\mathbf{f}_{mono}\Sigma_c \qquad \text{regime I} \tag{5a'}$$

If $\Sigma_{sat} > \Sigma_c$, as it is in practice, the condition of N for

regime II is that the slope of the pullout line must be smaller than that of the chain-scission line (thus, $N < \sigma_{craze}/\mathbf{f}_{mono}\Sigma_c$) but large enough that the stress to pull out the N block under saturation conditions will be greater than required for crazing (thus, $\sigma_{craze} < N\mathbf{f}_{mono}\Sigma_{sat}$). Therefore, the regime II the following condition must be satisfied:

$$\sigma_{craze}/\mathbf{f}_{mono}\Sigma_{sat} < N < \sigma_{craze}/\mathbf{f}_{mono}\Sigma_c \qquad \text{regime II} \qquad (5b)$$

Finally, if the slope of the pullout line is low enough, the crazing stress will not be reached at saturation and the conditions for regime III,

$$N < \sigma_{craze}/\mathbf{f}_{mono}\Sigma_{sat} \qquad \text{regime III} \qquad (5c)$$

will be satisfied.

Experimental Section

(1) **Materials.** PS and PVP homopolymers purchased from Aldrich Chemical Co., Inc., were of commercial grade with weight-average molecular weights of 250 000 and 200 000, respectively. The deuterated polystyrene/poly(2-vinylpyridine) (dPS/PVP) block copolymer used in this study was synthesized by anionic polymerization in tetrahydrofuran using cumylpotassium as the initiator at −55 °C in an argon atmosphere. The molecular weight and the composition of the block copolymer were characterized using gel permeation chromatography (GPC), forward recoil spectrometry (FRES),[18,19] and nuclear magnetic resonance (NMR). The polymerization indices of the dPS and the PVP blocks were respectively 580 and 220, and the polydispersity index was 1.05. More details of the polymerization and the characterization can be found elsewhere.[20] The PS block is deuterium labeled so that the quantity of the PS block at the interface can be analyzed with FRES.

The polymerization index of the dPS block is much larger than the polymerization index between entanglements, $N_{e;PS}$ (=173), ensuring that the dPS block can form entanglements with PS homopolymer. On the other hand, the polymerization index of the PVP block is 220 which is smaller than $N_{e;PVP}$ (=255).

(2) **Sample Preparation.** Slabs of PS and PVP were fabricated by compression molding at 160 °C. A thin film of the block copolymer was spun cast from a toluene solution on the PVP slab. The slab was dried at 80 °C, which is well below the T_g of PVP (108 °C), for 2 h in vacuum. This drying process does not induce the diffusion of block copolymer chains into PVP homopolymer. The areal density of block copolymer chains at the interface, Σ, was controlled by varying the concentration of the block copolymer in solution (0.1–1.3%), which determined in turn the thickness of the block copolymer layer; the Σ was measured with FRES. The resulting PVP slab was then joined to the PS slab, annealed in a mold at 160 °C for 2 h, and then allowed to cool to room temperature. In this annealing process, some block copolymer chains diffuse away from the interface but most block copolymer chains organize themselves at the interface and approach an equilibrium conformation; i.e., these copolymer chains strengthen the interface between the PS and PVP. The resulting sandwich was then cut with a diamond saw to obtain strips for the following fracture toughness measurement. The dimensions of the strips were 50.8 mm long × 8.7 mm wide × 4.0 mm thick (2.3 and 1.7 mm for PS and PVP, respectively). One of these strips was cut into smaller pieces for the microtomy described in a later section.

(3) **Fracture Toughness Measurement.** Fracture toughness of the interface, G_c, which is characterized by the critical energy release rate of an interfacial crack, was measured using an asymmetric double cantilever beam geometry.[5,6] The measurement was performed by inserting a single-edge razor blade, whose thickness is Δ, at the interface and pushing it into the interface at a constant rate of 3×10^{-6} m/s using a servo-controlled motor drive. The fracture toughness G_c was computed using

$$G_c = \frac{3\Delta^2 E_{PS} h_{PS}^3 E_{PVP} h_{PVP}^3}{8a^4}\left[\frac{E_{PS} h_{PS}^3 C_{PVP}^2 + E_{PVP} h_{PVP}^3 C_{PS}^2}{[E_{PS} h_{PS}^3 C_{PVP}^3 + E_{PVP} h_{PVP}^3 C_{PS}^3]^2}\right] \qquad (6)$$

where h_{PS} and E_{PS} denote the thickness and Young's modulus of the PS beam, respectively, and $C_{PS} = 1 + 0.64 h_{PS}/a$;[6] similar quantities are defined for PVP and labeled by the subscript PVP. The length a of the crack along the interface ahead of the razor blade was measured. To allow many measurements of a and thus G_c to be made, the entire history of the crack growth was recorded using a videocamera onto a videotape. The error bars reported subsequently for G_c represent ± 1 standard deviation of at least 16 measurements.

In the PS/PVP system, an asymmetric geometry is necessary to measure the true value of G_c of the interface. Since the modulus of PVP is higher than that of PS, the stress field near the crack tip is characterized by a complex stress intensity factor $K = K_1 + iK_2$, where $i = (-1)^{1/2}$. Specifically, the traction directly ahead of the crack tip along the interface has both a shear (σ_{xy}) and a tensile (σ_{yy}) component. The ratio of the shear stress to the tensile stress directly ahead of the crack tip at $x = d$, where d is a distance that is small compared to typical specimen dimensions, is related to a phase angle Ψ by

$$(\sigma_{xy}/\sigma_{yy})_{x=d} = \tan\Psi = \mathrm{Im}(Kd^{i\epsilon})/\mathrm{Re}(Kd^{i\epsilon}) \qquad (7)$$

where ϵ is a dimensionless material parameter which depends on mismatch of elastic moduli between the two materials on either side of the interface.[21] For the PS/PVP system $\epsilon = 0.0028$, which means that our phase angle Ψ depends negligibly on d. The energy release rate G, together with the phase angle Ψ, completely characterizes the stress field near the crack tip.

Cracks, and any crazes preceding them, tend to propagate toward a direction which minimizes the local σ_{xy} and thus Ψ. This tendency is especially pronounced for polymer/polymer interfaces when one polymer has a lower Young's modulus and a lower crazing stress than the other.[22]

At PS/PVP interfaces in symmetrically loaded specimens ($h_{PS} = h_{PVP}$), an interfacial crack and a craze would be driven toward the PS phase due to the Young's modulus mismatch, resulting in a larger G_c compared with that of the interface itself. We define such a phase angle as positive.

In order to measure the true value of G_c, the testing geometry must therefore have a small negative phase angle Ψ, which compensates the modulus mismatch and forces an interfacial crack to propagate at the interface. The asymmetric double cantilever beam geometry (thicker PS beam and thinner PVP beam) used in this study satisfies this small negative Ψ condition, ensuring that we will measure the G_c of the interface itself.

(4) **TEM Observation of Cracking of the Interface.**[11] We have combined a microtoming method[23] to produce thin films containing the interface and a copper grid technique[24] to allow such microtomed films to be strained in order to observe the fracture mechanisms at the interfaces by TEM.

A small piece of the strip containing the interface was microtomed so that the plane of the interface was perpendicular to the section and the direction of cutting was parallel to the line of intersection between the interface and the cutting plane to obtain thin (0.5–1.0-μm) films. Wrinkles in the film caused by microtoming were removed by briefly exposing the film to solvent (toluene/chloroform = 50/50) vapor. The resulting film was then bonded to a ductile copper grid (1 × 1 mm grid squares), the grid bars of which had been previously coated with PS/PVP block copolymer (PS/PVP = 960/950), by exposing the film to the vapor of the same solvent mixture for several seconds to ensure good bonding between the grid bars and the film. The film was then dried at 50 °C for 12 h in vacuum to evaporate the solvents and to relax the residual stress.

The resulting grid was strained in tension at a constant strain rate of $\sim 4 \times 10^{-4}$/s with a servo-controlled motor drive at room temperature in air. With this strain rate, the craze interface velocity (which is approximately proportional to, but less than,

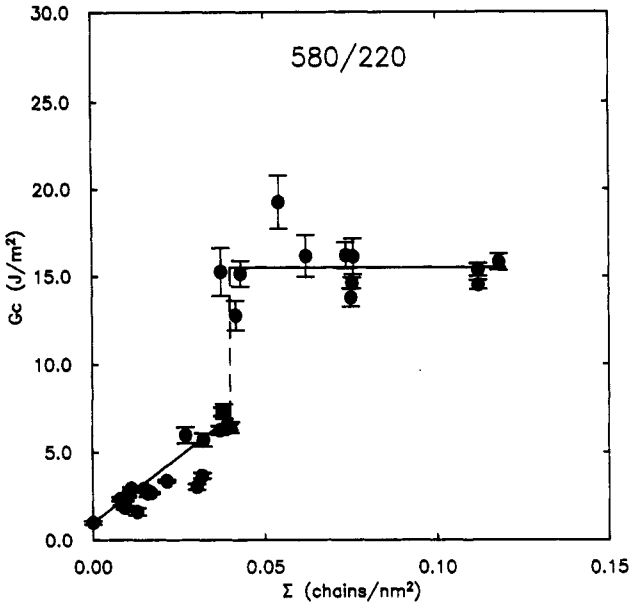

Figure 2. Fracture toughness G_c as a function of Σ. Note that a discontinuous transition in G_c at Σ^* is observed. Below the transition, G_c increases linearly with Σ, whereas, above the transition, G_c remains constant.

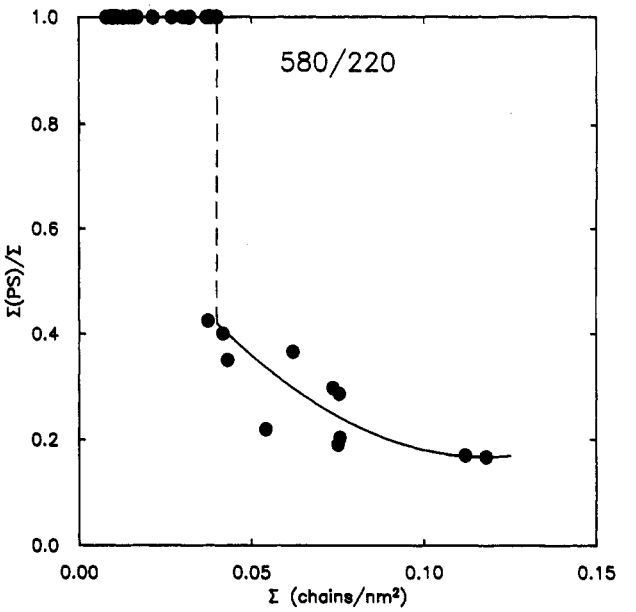

Figure 3. Fraction of the dPS block found on the PS side of the fracture surface as a function of Σ. This plot also exhibits a discontinuous decrease at Σ = 0.04 chains/nm^2.

the crack velocity) of this TEM experiment is very close to that of the fracture toughness measurement. The plastic deformation of the copper grid ensures that the strain in the polymer film was retained during the TEM observation. The film was then exposed to iodine vapor at room temperature for 3 h to stain the PVP phase in the film for the TEM observation. PVP forms a complex with iodine,[25] while PS does not, resulting in enhanced electron scattering from, and hence a "darkening" of, the PVP phase which can then be easily distinguished from the less scattering, "brighter" phase of PS. The grid bars surrounding those of a selected square were carefully cut with a razor blade, and then the film was observed with a (JEOL Model 1200EX) transmission electron microscope operating at 120 keV. More details of this technique can be found elsewhere.[11]

Results

(1) G_c Measurements. In Figure 2, G_c is plotted as a function of Σ, and it is clear that a discontinuous transition took place at Σ = 0.040 chains/nm^2. For Σ < 0.040 chains/nm^2, G_c linearly increased with increasing Σ; at Σ = 0.040 chains/nm^2, G_c showed a jump by about 10 J/m^2 and hereafter remained approximately constant for higher values of areal density.

(2) Fracture Analysis. After the G_c measurement, the halves of the fracture surfaces were examined by FRES to determine the areal density of block copolymer chains (based on the areal density of the dPS block) on both PS and PVP sides (Σ(PS) and Σ(PVP), respectively). The total areal chain density, Σ, was calculated by summing these two measurements.

Figure 3 shows the fraction of the dPS block found on the PS side, i.e., Σ(PS)/Σ, as a function of Σ. Here also it was found that a clear transition took place at Σ = 0.040 chains/nm^2. For Σ < 0.040 chains/nm^2, all dPS blocks of block copolymer chains organized at the interface before fracture were found on the PS side of the fracture surface. In contrast, for Σ > 0.040 chains/nm^2, most of the dPS block of the block copolymer chains was found on the PVP side of the fracture interface.

(3) TEM Analysis. Figure 4a shows a crack at the interface at a Σ (=0.0087 chains/nm^2) below the transition value of 0.04 chains/nm^2, where one can see no craze or other plastic deformation ahead of the crack tip. In contrast to the case for low Σ, above the transition (Σ = 0.048 chains/nm^2), fracture took place after a craze had widened as shown in Figure 4b, where a craze precedes the crack at the interface. The locus of the fracture was at the PVP/PS–craze interface, indicating that the interface is still the weakest point in the material. Similar results were reported[11] earlier for PS/PVP interfaces reinforced with different dPS/PVP block copolymers with long PVP blocks.

Discussion

(1) Fracture Mechanisms of the Interface. In this section we will identify the type of transition observed in both G_c and the distribution of block copolymer chains on the fracture surfaces.

From the results of Figures 3 and 4a, one cannot tell which fracture mechanism is active below the transition; both chain scission and chain pullout can, in principle, explain these two results. The linear dependence of G_c on Σ below the transition, however, strongly suggests that the fracture mechanism of the interface in this regime is one-sided chain pullout.[9] In addition, the polymerization index of this PVP block is lower than $N_{e;PVP}$, also suggesting the chain pullout mechanism. If chain scission were the mechanism of interface failure, one would not expect scission to occur exactly at the joint between the blocks for all copolymer chains: indeed previous studies of the PS/PVP system[6] showed that most, but not all, of the dPS block is located on the PS side of the fracture surface in the low Σ, chain-scission, regime. The fact that *all* the dPS is on the PS side below Σ^* = 0.04 chains/nm^2 for the 580/220 block copolymer strongly indicates that the failure mechanism here is pullout. Furthermore, from the previous studies on the bond fracture force,[6,7,16,17] the chain-scission force, f_b, for the C–C bond is reported to be around 2.2 × 10^{-9} N/bond. This estimate yields Σ_c to be 0.025 chains/nm^2 from eq 3, which is lower than the transition observed in this study, and thus the chain scission/crazing transition can be eliminated as a possibility for the transition we observe.

On the other hand, the fracture mechanism for Σ > Σ^* is undoubtedly crazing as shown by the TEM results (see Figure 4b). However, in the crazing regime, G_c should scale as $G_c \sim \Sigma^2$, although we found G_c remained

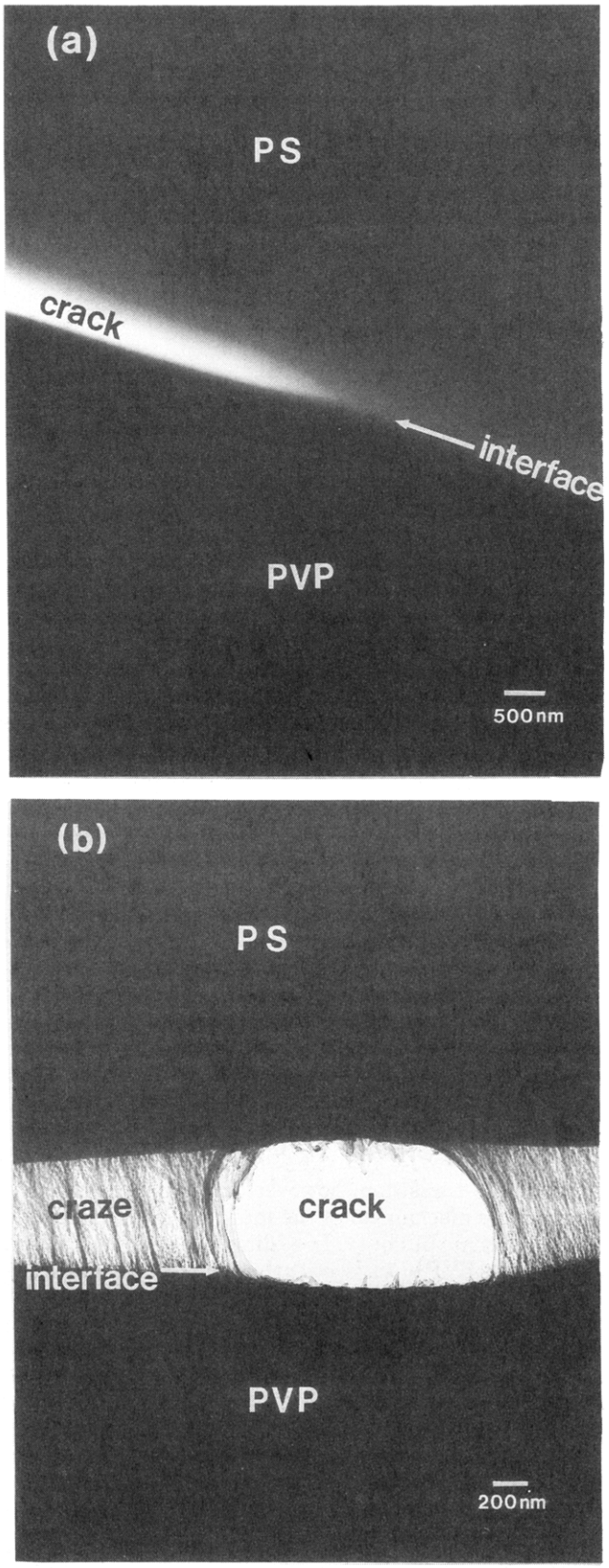

Figure 4. TEM micrographs showing a crack at the interface: (a) Σ = 0.0087 chains/nm^2 (below the transition) and (b) Σ = 0.048 chains/nm^2 (above the transition). Note that no craze can be seen in a, while in b a craze in the PS phase preceded the crack and the locus of the fracture is within the craze, but close to the PS/PVP interface.

approximately constant for 580/220 block copolymer over the entire range of crazing. In addition, Creton et al.[6] and Washiyama et al.[15] showed that G_c increased with increasing Σ for a 510/540 block copolymer (similar length of the dPS block with a longer PVP block to the 580/220 block copolymer). We believe that these results are due to the fact that some of PVP blocks of the 580/220 block copolymer pull out of the PVP side of the interface during craze growth.

From Figure 3, 20–40% of the total dPS block of the block copolymer was found on the PS side in the crazing regime. Creton et al.,[6] however, reported that when craze breakdown occurred in the block copolymer brush, only 5–10% of the dPS block of the dPS/PVP (for 510/540 and 800/870) block copolymer was observed on the PS side of the fracture surfaces, provided that both PS and PVP blocks entangled firmly with its respective homopolymer. This comparison therefore indicates that, for the 580/220 system, the craze fractured both by chain scission at the dPS block brush/PS homopolymer interface and by chain pullout of the PVP block from the PVP bulk; the latter mechanism produces a higher value of Σ(PS)/Σ than does the former mechanism. Once a craze or a crack is formed, a stress concentration is developed near the craze or crack tip,[7,8] and hence this stress concentration is able to cause chain pullout of the PVP block from the PVP bulk, when the stress near the craze or crack tip exceeds the chain pullout stress, $\sigma_{pullout}$. (We cannot rule out *some* contribution to the craze fracture from dPS block pullout. The reasoning above, however, suggests that it cannot be a dominant contribution to the 580/220 craze fracture.)

Since block copolymer chains which are pulled out from the PVP bulk can no longer contribute to craze strength, only the remaining areal strand density, $\Sigma_{eff}' = \Sigma_{eff} - \Sigma_{pullout}$, can contribute to the craze strength and thus G_c. Σ_{eff} denotes the number of effectively entangled chains defined by Creton et al. and can be evaluated using a self-consistent mean-field (SCMF) theory.[6] $\Sigma_{pullout}$ corresponds to the areal density of those chains which pull out from the PVP bulk during craze propagation and, hence, cannot contribute to G_c. These quantities are shown as a function of Σ in Figure 5a; $\Sigma_{pullout}$ = Σ(PS) − 0.005 chains/nm^2, where Σ(PS) is the (experimental) areal density of the dPS block on the PS side of the fracture surface and the offset of 0.005 accounts for the dPS found on the PS side of the fracture surface in the case where no PVP block chains are pulled out and the dPS block is about the same length (e.g., in the 510/540 block copolymer[6,15]). The fracture toughness will scale as $G_c \sim \Sigma_{eff}'^2$. As shown in Figure 5b, Σ_{eff}' does not change much in the range of 0.04 < Σ < 0.12 chains/nm^2. The fact that G_c measured experimentally remained constant in this range of Σ is therefore not surprising.

This result indicates that the craze breakdown mechanism depends on N_{PVP}. For short N_{PVP}, chain pullout will be the dominant mechanism of craze breakdown, and in this case G_c scales as $G_c \sim \Sigma$.[6] On the other hand, for long N_{PVP}, chain scission can be dominant, where G_c scales as $G_c \sim \Sigma^2$. This second case is important to achieve large G_c, and we will discuss the critical value of N_{PVP} in the next section.

(2) The Static Monomer Friction Coefficient of PVP Monomers. The static friction coefficient of PVP per monomer, f_{mono}, is an important parameter governing the fracture mechanism map. One can calculate f_{mono} if Σ^* is known. In this case, one can use the crazing stress of PS for σ_{craze}, since the interfacial craze propagated in the PS. Inserting Σ^* = 0.040 chains/nm^2, σ_{craze} = 55 MPa at the appropriate strain rate,[6] and N_{PVP} = 220 into eq 4, one obtains $f_{mono} = 6.3 \times 10^{-12}$ N/monomer. It should be noted however that this value is expected to depend strongly on the experimental conditions, such as temper-

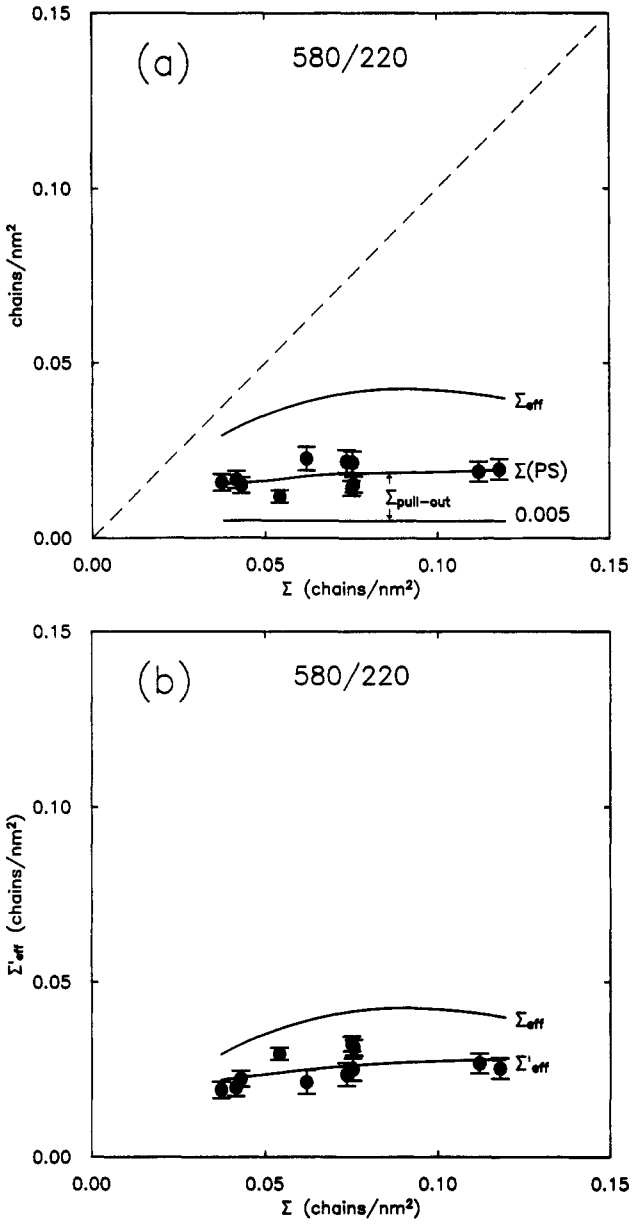

Figure 5. Areal density of block copolymer chains contributing to craze strength: (a) Σ_{eff} (from SCMF calculation), Σ(PS) (from measurements of dPS on the PS side of the fracture surface), and $\Sigma_{pullout} = \Sigma(PS) - 0.005$ (see text); (b) Σ_{eff}' as a function of Σ, the total areal density of the block copolymer at the interface. Note that Σ_{eff}' has a very weak dependence on Σ in the range of $0.040 < \Sigma < 0.12$ chains/nm^2.

ature, environment, and perhaps strain rate at higher values.

The dependence of f_{mono} on temperature and strain rate and, more precisely, the constitutive law of the pullout process are quite important issues for the deformation and fracture of glassy polymers.[26,27] The present experimental method can be used to determine the friction coefficients of polymer chains in the glassy state, both for the block of the same type as the homopolymer, i.e., A in A, and for the block in a miscible homopolymer of different chemical architecture, i.e., A in C.

(3) Restricting Conditions for the Regime II. Regime II only occurs when the product $f_{mono}N_{PVP}$ is between the upper and lower limits set by eq 5b. These limits dictate the boundaries between regimes I and II and between regimes II and III, respectively. In this section, we will discuss these boundaries (Table I).

Regime I to Regime II Boundary. The boundary between regime I and regime II is dictated by the product

Table I. Summary of the Fracture Mechanism Map

regime	conditions		fracture mechanism
I	$N > \sigma_{craze}/f_{mono}\Sigma_c$	$\Sigma < \Sigma_c$	chain scission
	$\Sigma_c = \sigma_{craze}/f_b$	$\Sigma > \Sigma_c$	crazing
II	$\sigma_{craze}/f_{mono}\Sigma_{sat} < N < \sigma_{craze}/f_{mono}\Sigma_c$	$\Sigma < \Sigma^*$	chain pullout
	$\Sigma^* = \sigma_{craze}/f_{mono}N$	$\Sigma > \Sigma^*$	crazing
III	$N < \sigma_{craze}/f_{mono}\Sigma_{sat}$	$\Sigma < \Sigma_{sat}$	chain pullout

$f_{mono}N_{PVP}$ as shown in eq 5a,b, so that it is useful to estimate the critical polymerization index, N^*, of PVP, above which no chain pullout can take place, corresponding to regime I. It should also be emphasized that this parameter N^* is very important for the molecular design of block copolymers for the toughening of polymer/polymer interfaces. With an additional condition of $\Sigma^* = \Sigma_c$, eqs 3 and 4 can be recast to

$$N^* = f_b/f_{mono} \tag{8}$$

With $f_b = 2.2 \times 10^{-9}$ N/bond and $f_{mono} = 6.3 \times 10^{-12}$ N/monomer, one obtains $N^* = 350$, which is larger than $N_{e;PVP}$ (=255) but less than $2N_{e;PVP}$, corresponding to the crossover regime of entanglements, where some chains can form entanglements, while others cannot. It should be noted that this estimate is valid only when the friction stress is given by eq 2. However, any localized extra friction at an entanglement (which is this context might be visualized as a tight interlocking loop) would drastically increase the friction stress and hence result in a stronger power law than eq 2. This effect will result in a smaller value of N^*, one closer to $N_{e;PVP}$.

Regime II to Regime III Boundary. One can estimate the critical polymerization index, N^{**}, for this boundary by combining eq 4 and an additional condition of $\Sigma^* = \Sigma_{sat}$, yielding eq 9.

$$N^{**} = \sigma_{craze}/f_{mono}\Sigma_{sat} \tag{9}$$

Here, Σ_{sat} is restricted by micelles or lamellar layer formation near the interface, which is determined in turn by thermodynamic characteristics of the system, particularly the segregation isotherm,[14] and φ_{cmc}, a critical micelle concentration,[12] which can be estimated by using FRES and TEM.[28] It should be noted that Σ_{sat} is not a constant but depends on N_{PVP} and N_{dPS}. For large N_{dPS}, however, Σ_{sat} has only a weak dependence on N_{PVP} and Σ_{sat} slightly decreases with increasing N_{PVP}.[13] In our system, $N_{dPS} \sim 600$ will meet this large N_{dPS} condition and thus we assume Σ_{sat} to be constant: Σ_{sat} does not depend on N_{PVP}. Under this assumption, N^{**} will be slightly overestimated due to the dependence of Σ_{sat} on N_{PVP}. Using TEM, one can determine Σ_{sat} beyond which micelles can be recognized near the interface. From the TEM experiment Σ_{sat} is estimated to be 0.11 chains/nm^2, and thus one obtains $N^{**} \sim 80$. This value is reasonable and consistent with other studies. For the dPS/PVP block copolymer of 625/49, no crazing was observed;[6] on the other hand, from TEM studies, for the 680/100 block copolymer, the formation of a small craze at the interface was reported,[11] which is consistent with the present estimation of N^{**}.

Conclusions

We have investigated fracture toughness, G_c, and fracture mechanisms of planar interfaces between PS and PVP, which are reinforced with a dPS/PVP block copolymer of 580/220, in order to examine the fracture mechanism map,[9] particularly the fracture mechanism transition from chain pullout to crazing.

We have observed a transition in both the fracture mechanism and G_c which occurs at $\Sigma^* = 0.04$ chains/nm^2. Below the transition the fracture mechanism is chain pullout of the PVP block from the PVP bulk. Above the transition, the mechanism is crazing, followed by craze breakdown at the interface. At the transition, G_c shows a discontinuous jump by $\sim$10 J/m^2.

Using this transition value of Σ^*, we have estimated the static friction coefficient per monomer of PVP to be $\mathbf{f}_{mono} = 6.3 \times 10^{-12}$ N/monomer. The existence of the fracture mechanism transition from chain pullout to crazing is restricted by upper and lower limits of the polymerization index of the PVP block, which are estimated to be 350 and 80, respectively; the former would be overestimated and thus closer to $N_{e;PVP}$ (=255) due to strong friction at an entanglement.

This experimental method for obtaining the static friction coefficient per monomer, $\mathbf{f}_{mono}$, which is a particularly important parameter to describe crazing and fracture of glassy polymers, should be applicable to a variety of polymers.

Acknowledgment. We gratefully acknowledge that this work was carried out as part of a project of the Cornell Materials Science Center (MSC) which is funded by the National Science Foundation and benefited from the use of MSC Central Facilities. We also appreciate stimulating discussions with C. Creton and K. H. Dai and the important contributions of C. Creton in the synthesis of the block copolymer. J.W. is supported by a grant from Showa Denko K.K., Japan.

References and Notes

(1) Fayt, R.; Jérôme, R.; Teyssié, Ph. *J. Polym. Sci., Polym. Phys. Ed.* **1989**, *27*, 775.
(2) Fayt, R.; Teyssié, Ph. *Polym. Eng. Sci.* **1989**, *29*, 538.
(3) Creton, C.; Kramer, E. J.; Hadziioannou, G. *Macromolecules* **1991**, *24*, 1846.
(4) Cao, H. C.; Dagleish, B. J.; Evans, A. G. *Closed Loop* **1990**, *23*, 3929.
(5) Brown, H. R. *Macromolecules* **1989**, *22*, 2859.
(6) Creton, C. Ph.D. Thesis, Cornell University, Ithaca, NY, 1992. Creton, C.; Kramer, E. J.; Hui, C. Y.; Brown, H. R. *Macromolecules* **1992**, *25*, 3075.
(7) Brown, H. R. *Macromolecules* **1991**, *24*, 2752.
(8) Hui, C. Y.; Ruina, A.; Creton, C.; Kramer, E. J. *Macromolecules* **1992**, *25*, 3948.
(9) Xu, D. B.; Hui, C. Y.; Kramer, E. J.; Creton, C. *Mech. Mater.* **1991**, *11*, 257.
(10) Brown, H. R.; Deline, V. R.; Green, P. F. *Nature* **1989**, *341*, 221.
(11) Washiyama, J.; Creton, C.; Kramer, E. J. *Macromolecules* **1992**, *25*, 4751.
(12) Shull, K. R.; Kramer, E. J.; Hadziioannou, G.; Tang, W. *Macromolecules* **1990**, *23*, 4780.
(13) Shull, K. R.; Kramer, E. J. *Macromolecules* **1990**, *23*, 4769.
(14) Dai, K. H.; Kramer, E. J.; Shull, K. R. *Macromolecules* **1992**, *25*, 220.
(15) Washiyama, J.; Creton, C.; Kramer, E. J.; Xiao, F.; Hui, C. Y. *Macromolecules*, submitted for publication.
(16) Kausch, H. H. In *Polymer Fracture*, 2nd ed.; Springer Verlag: Berlin, 1987.
(17) Odell, J. A.; Keller, A. *J. Polym. Sci., Polym. Phys. Ed.* **1986**, *24*, 1889.
(18) Feldman, L. C.; Mayer, J. W. In *Fundamentals of Surface and Thin Film Analysis*; North-Holland: Amsterdam, The Netherlands, 1986.
(19) Mills, P. J.; Green, P. F.; Palmstrom, C. J.; Mayer, J. W.; Kramer, E. J. *J. Appl. Phys. Lett.* **1984**, *45*, 958.
(20) Shull, K. R. Ph.D. Thesis, Cornell University, Ithaca, NY, 1990.
(21) Rice, J. R. *J. Appl. Mech.* **1988**, *55*, 98.
(22) Brown, H. R. *J. Mater. Sci.* **1990**, *25*, 2791.
(23) Beahan, P.; Bevis, M.; Hull, D. *Philos. Magn.* **1971**, *24*, 1267.
(24) Lauterwasser, B. D.; Kramer, E. J. *Philos. Magn.* **1979**, *A39*, 469.
(25) Aronson, S.; Wilensky, S. B. *J. Polym. Sci., Polym. Chem. Ed.* **1988**, *26*, 1259.
(26) Kramer, E. J. *Adv. Polym. Sci.* **1983**, *52/53*, 1.
(27) Kramer, E. J.; Berger, L. L. *Adv. Polym. Sci.* **1990**, *91/92*, 1.
(28) Shull, K. R.; Winey, K. I.; Thomas, E. L.; Kramer, E. J. *Macromolecules* **1991**, *24*, 2748.